Molecular Hydrophobicity of Hydroxylated MgO Surfaces

Narendra M. Adhikari[1]*, Aashish Tuladhar[1], Zheming Wang[1], James J. De Yoreo[1,2], and Kevin M. Rosso[1]*

[1] Physical Sciences Division, Physical and Computational Sciences Directorate, Pacific Northwest National Laboratory, Rich-land, Washington 99352, United States
[2] Department of Materials Science and Engineering, University of Washington, Seattle, WA 98195, United States

***Corresponding authors**

Narendra M. Adhikari
narendra.adhikari@pnnl.gov
Kevin M. Rosso
kevin.rosso@pnnl.gov

Cleaning of the MgO Single Crystal Substrates for the vSFG Experiment

The single crystal MgO substrates for the vSFG experiment were cleaned to ensure the removal of the adsorbed hydrocarbons from the surfaces. The substrates after taking out from manufacturer's packing were rinsed with the DI water, dried by blowing air and then treated with the UV irradiation for about 30 minutes. The substrates were then plasma cleaned (Harrick plasma cleaner (Ithaca, NY USA) for about five minutes. The vSFG spectra was recorded at each stages of the cleaning of the substrate. This is an important step in surface preparation protocol because the presence of the adsorbed hydrocarbons can alter the hydrophilicity/hydrophobicity of the surface.[1] Figure S1 shows the vSFG spectra from the substrates before and after cleaning with the deionized water and subsequent UV irradiation for 30 minutes and finally after plasma cleaning for about five minutes. The inset shows the spectra in the C-H stretching region. The vSFG spectra from the as received substrate show hydrocarbon residue (2800-3000 cm^{-1}) present on the surface which is diminished after the washing and UV treatment and completely removed by the plasma cleaning.

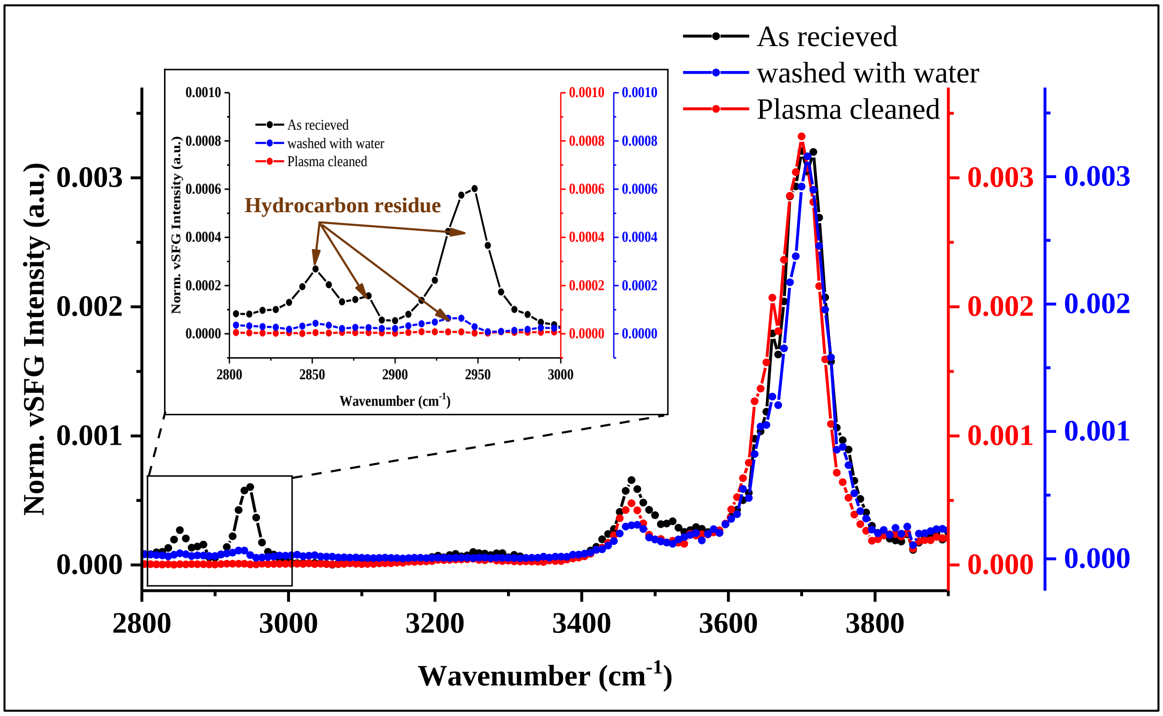

Figure S1. vSFG spectra from Air/MgO(100) interface in SSP polarization combination. Spectra were recorded for the as received sample immediately after opening the packing from the vendor (black spectrum). The substrates were cleaned with the deionized water and treated with UV irradiation for 30 minutes (blue spectrum) and finally after plasma cleaning for about five minutes (red spectrum). The inset shows the spectra in the C-H stretching region.

Fitting Parameters at the air-MgO Interfaces

Tables S1-S2 contains the fitting parameter with the standard error obtained from the fitting of the vSFG spectra at the air/MgO interface for the MgO(100) and MgO(111) interfaces.

Table S1. Fitting parameter for the Air/MgO(100) spectrum

Air/MgO(100)	y_0		x_c		ω		A	
	Value	Standard Error	Value	Standard Error	Value	Standard Error	Value	Standard Error
Peak1	-0.001	0.007	3445	7	28	11	9	3
Peak2	-0.001	0.007	3638	7	33	5	20	5
Peak3	-0.001	0.007	3689	4	34	5	32	5
Reduced χ^2		1.7E-03		Adjusted R^2		0.970		

Table S2. Fitting parameter for the Air/MgO(111) spectrum

Air/MgO(111)	y_0		x_c		ω		A	
	Value	Standard Error	Value	Standard Error	Value	Standard Error	Value	Standard Error
Peak1	-0.002	0.005	3430	63	27	93	3	8
Peak2	-0.002	0.005	3627	7	23	10	7	3
Peak3	-0.002	0.005	3712	1	34	2	32	1
Reduced χ2		1.0E-03		Adj. R2		0.975		

vSFG spectra of the MgO/water interface

A homemade sample cell as shown in Figure S2 with the inlet and outlet for liquid was used for the vSFG studies at the solid-liquid interface. The MgO substrate is at the top and is in contact with the bulk of D_2O.

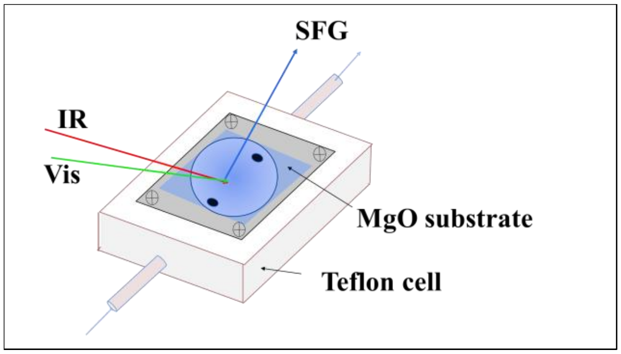

Figure S2. Schematic of the sample cell used for vSFG experiment

The vSFG spectra were collected from the MgO(100) surfaces in contact with liquid H_2O and liquid D_2O, focusing on the OH and OD stretching regions. D_2O was particularly useful as an alignment tool to ensure the vSFG spectra recorded indeed are generated from the MgO/liquid interface of interest (i.e., as opposed to the MgO/air interface on the back side of the slab). The use of D_2O enabled us to distinguish between the surface hydroxyl groups on the air side (OH groups) from the hydroxyl groups on the liquid side (OD groups) of the sample. Hence, we ensure that the vSFG signal recorded is free from that of the air/MgO interface, as shown in Figure S3 A. (Note that the dips observed in the 2360-2390 cm^{-1} region (Figure S3 B) are due to IR absorption by atmospheric CO_2 in the D_2O.) As seen in Figure S3 A, the intensity at the MgO/H_2O interface is weaker compared to that of the air/MgO interface. This is due to the reduced interfacial Fresnel factor as well as the experiment being performed in such a way that both the incident beams as well as generated SFG must pass through the MgO substrate. The resulting near-zero intensity in the OH stretching region when D_2O is introduced in place of H_2O ensures that proper alignment is attained during the vSFG experiments.

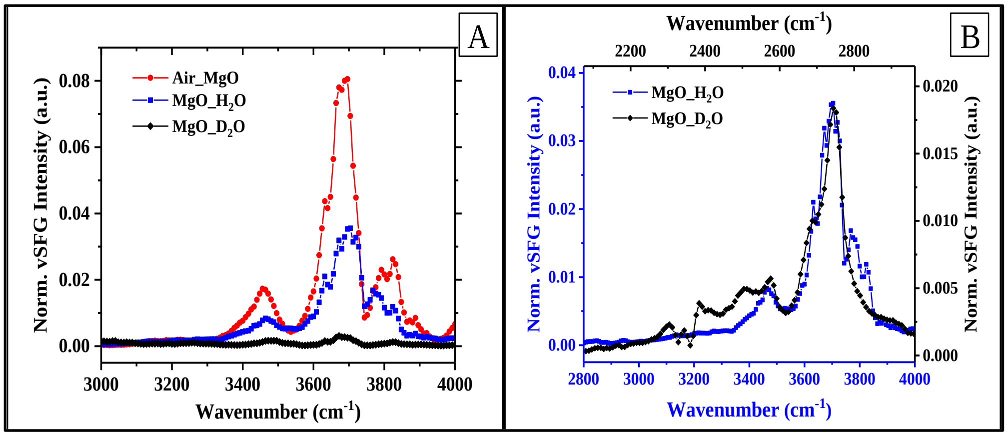

Figure S3. vSFG spectra in SSP polarization combination from the MgO(100)/water interface. **A.** Comparison of the vSFG spectra from the Air-MgO, MgO-H_2O, and MgO-D_2O interfaces in the OH stretch frequency region; **B.** Comparison of the normalized vSFG spectra from the MgO(100)-H_2O interface in the OH stretching region (bottom and left axes) and MgO(100)-D_2O interface in the OD stretching region (top-right axes).

The reference spectra were also recorded from the IR grade fused silica/D_2O and Al_2O_3(0001)/D_2O interfaces using the same optical geometry. Figure S4 A shows the comparison of the vSFG signal from the MgO(100)/D_2O and IR grade fused silica/D_2O and Al_2O_3(0001)/D_2O interfaces in the OD stretching region. These spectra from the silica/D_2O and Al_2O_3(0001)/D_2O interfaces resemble the spectra reported in the literature.[2-6] The vSFG signature from the fused silica is dominated by the H-bonded OD vibrational stretching modes (2250-2650 cm^{-1}) with no non-H-bonded OD peak, whereas for MgO(100), vSFG spectra are dominated by a strong non-H-bonding OD stretching mode (~2750 cm^{-1}), with shallower H-bonding OD stretching modes. Figure S4 B compares the data collected in SSP polarization combination of the IR grade fused silica/water to the SSP data from the plasma cleaned silica/water at pH 6 reported by Dalstein *et.al*.[6]

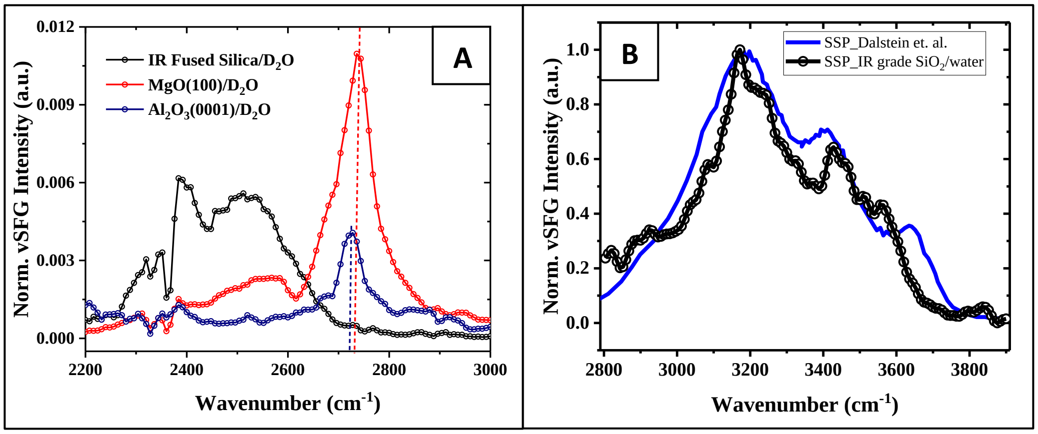

Figure S4. A. Comparison of the vSFG intensity in SSP polarization combination from the MgO(100)/D_2O, IR grade fused silica/D_2O and Al_2O_3(0001)/D_2O interfaces. All the spectra were recorded with the flat optical geometry and are normalized separately by the power of the incident laser beams. The sensitivity of the photomultiplier tube (PMT) used was kept constant during spectra collection to allow direct intensity comparison. **B.** Comparison of the normalized vSFG data recorded from the fused silica/water interface with that of the Dalstein et. al.[6]

The Al_2O_3(0001)/D_2O interface shows a weak non-bonding OH stretching mode with very weak H-bonding OH stretching modes. Also, the non-bonded OD stretch in the MgO(100) /D_2O interface is blue shifted by about 15 cm^{-1} compared to that in the Al_2O_3(0001)/D_2O interface.Figure S3 B compares the vSFG spectra from the MgO/H_2O and MgO/D_2O interfaces collected in the OH and OD stretching region, respectively. When normalized for peak shifting corresponding to the isotopic dilution factor of 1.35 for H/D exchange, the spectra from MgO/H_2O and MgO/D_2O interfaces have similar spectral features, except that there is a slight increase in intensity in the H-bonded OD stretching region at a lower frequency (~2300-2600 cm^{-1}).

Time Dependent vSFG Experiment for the MgO(100)/D_2O interface.

Time dependent vSFG measurements were recorded from the MgO(100)/D_2O interface to ensure the MgO surface does not change during the experiment due to solubility in water. The vSFG intensity of the non-H-bonded (2745 cm^{-1}) and H-bonded (2500 cm^{-1}) OD stretching modes in SSP polarization combination from the MgO(100)/D_2O interface were recorded as a function of time up to five hours. Also, the SSP spectrum was recorded before and after time dependent experiments as shown in Figure S5.

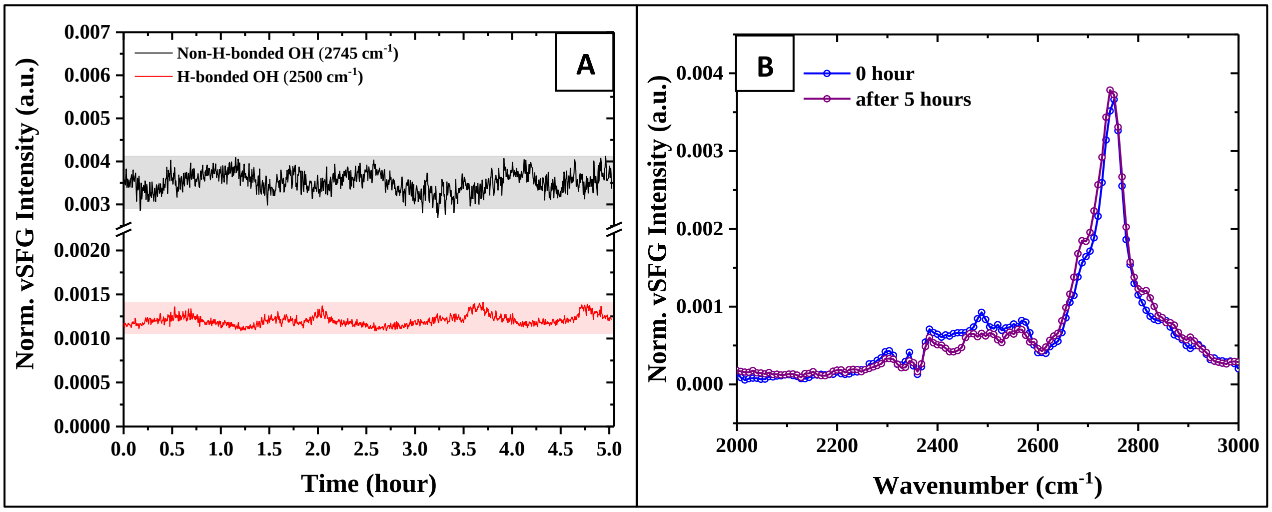

Figure S5. A. The time dependent vSFG intensity of the Non-H-bonded and H-bonded OD vibrational modes in SSP polarization combination from the MgO(100)/D_2O. Each data point is the average of over 50 laser shots (repetition rate of 10 Hz) and normalized by the power of the incident laser beams. **B.** The vSFG spectra from the MgO(100)/D_2O interface at the beginning and the end of the time dependent experiment on the **A**.

The time dependent vSFG experiment shows no appreciable change in the surface structure of the MgO during an extended period.

Fitting Parameters at the MgO/D_2O interfaces

Tables S3-S4 contains the fitting parameter with the standard error obtained from the fitting of the vSFG spectra at the MgO/D_2O interfaces for the MgO(100) and MgO(111) interfaces.

Table S3. Fitting parameter for the MgO(100)/D2O spectrum

MgO(100)/D_2O	y_0		x_c		ω		A	
	Value	Standard Error	Value	Standard Error	Value	Standard Error	Value	Standard Error
Peak1	0.004	0.004	2454	7	252	22	87	7
Peak2	0.004	0.004	2685	3	67	4	41	3
Peak3	0.004	0.004	2733	2	28	4	17	3
Reduced χ^2	6.1E-04		Adjusted R^2		0.987			

Table S4. Fitting parameter for the MgO(111)/D2O spectrum

MgO(111)/D_2O	y_0		x_c		ω		A	
	Value	Standard Error	Value	Standard Error	Value	Standard Error	Value	Standard Error
Peak1	0.030	0.006	2424	17	200	44	50	10
Peak2	0.030	0.006	2685	4	60	11	26	5
Peak3	0.030	0.006	2752	2	28	3	21	2
Reduced χ^2	1.4E-03		Adjusted R^2		0.951			

Polarization-dependent vSFG spectra

vSFG spectra were recorded in SSP and PPP polarization combination. The abbreviations SSP and PPP indicate the polarization state of the SFG, Visible, and IR beam in the decreasing order of frequency of the beams. S-polarized beam has the electric field along x- and y-axes whereas the P-polarized beam contains the electric field only along the z-axis. Figures S6 shows the SSP and PPP spectra collected for the MgO(100) and MgO(111) in the air and contact with the D_2O. The PPP spectra have significantly larger intensities for the MgO(111) crystal.

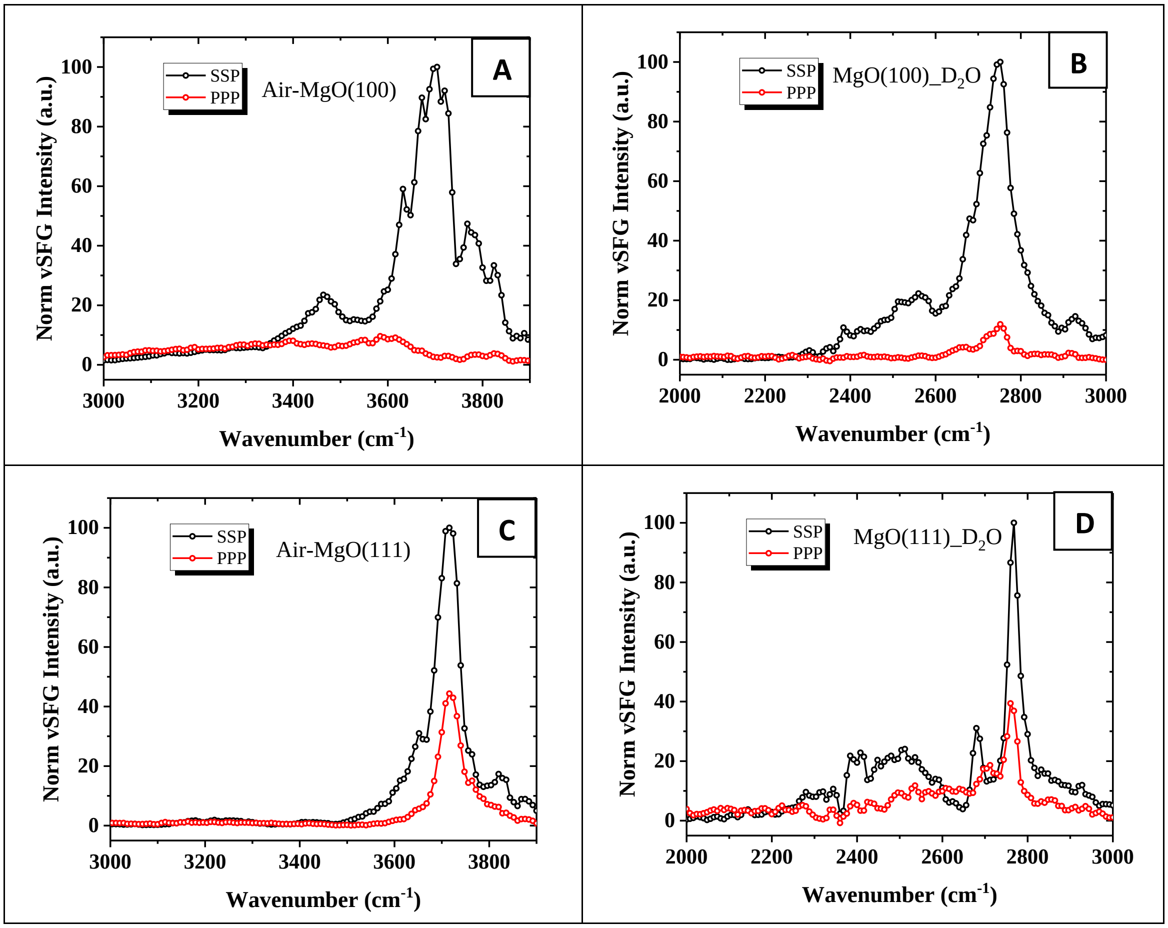

Figure S6. SSP and PPP spectra from the **A.** Air-MgO(100), **B.** MgO(100)/D_2O, and **C.** Air-MgO(111), and **D.** MgO(111)/D_2O interfaces.

Water contact angle (WCA) Measurements

The water contact angle (WCA) of the single-crystal MgO substrates were measured with a home-built goniometer using a USB microscope (Opti-Tekscope, China). The contact angles of the plasma cleaned MgO(100) and MgO(111) surfaces were measured. Also, similar measurements were performed for the plasma cleaned Al_2O_3(0001) and IR grade fused silica substrates. The images were analyzed with ImageJ[7] with a low-bond axisymmetric drop shape analysis (LB-ADSA) plugin.[8] Multiple measurements with multiple substrates were performed to minimize the error of the contact angle obtained. Figure S5 shows the example snapshots of the images of the water droplet on the MgO single crystal surfaces before and after cleaning of the substrates. Figure S7 shows the snapshots of the water droplet on the as received and plasma cleaned MgO single crystal surface along with that for the plasma cleaned Al_2O_3(0001) and IR grade fused silica substrates. The contact angle of the plasma cleaned fused silica was beyond the minimum limit (WCA ~10^o) of the software employed.

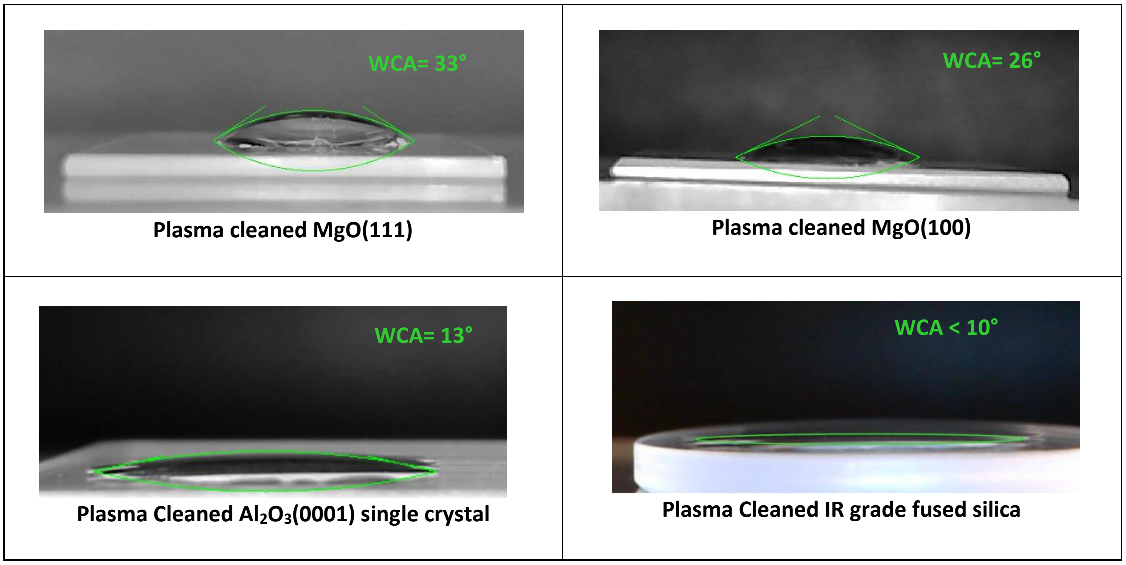

Plasma cleaned MgO(111)

Plasma cleaned MgO(100)

Plasma Cleaned Al_2O_3(0001) single crystal

Plasma Cleaned IR grade fused silica

Figure S7. Snapshots of the water droplet on the MgO single crystal surface before and after plasma cleaning. The contact angle of the plasma cleaned fused silica was beyond the minimum limit (WCA ~10^o) of the LB-ADSA plugin used to determine WCA.

The water contact angle (WCA) for the plasma cleaned MgO(100) and MgO(111) surfaces (WCAs of 26±1° and 33±2°, respectively) were higher than that for the plasma cleaned Al_2O_3(0001) (WCA = 13±1°) and IR grade fused silica (WCA < 10°). The contact angles obtained for the MgO single crystals were lower than those predicted for anhydrous MgO surfaces,[9,10] however, the contact angle values for the silica and alumina substrate agree well with the literature values.[4,11] Moreover, the measured WCA values are correlated with the intensity and the peak position of the non-H-boning OH stretching modes. The contact angle follows the order MgO > Al_2O_3 > fused silica whereas the non-bonding OH group intensity follows the order MgO >Al_2O_3 >> fused silica. The stretching vibrational frequency of the non-H-bonding OH groups follows the order MgO(111) > MgO(100) > Al_2O_3(0001).

References

1 Zubkov, T. *et al.* Ultraviolet Light-Induced Hydrophilicity Effect on TiO2(110)(1×1). Dominant Role of the Photooxidation of Adsorbed Hydrocarbons Causing Wetting by Water Droplets. *The Journal of Physical Chemistry B* **109**, 15454-15462, doi:10.1021/jp058101c (2005).

2 Tuladhar, A., Piontek, S. M. & Borguet, E. Insights on Interfacial Structure, Dynamics, and Proton Transfer from Ultrafast Vibrational Sum Frequency Generation Spectroscopy of the Alumina(0001)/Water Interface. *The Journal of Physical Chemistry C* **121**, 5168-5177, doi:10.1021/acs.jpcc.7b00499 (2017).

3 Zhang, L., Tian, C., Waychunas, G. A. & Shen, Y. R. Structures and Charging of α-Alumina (0001)/Water Interfaces Studied by Sum-Frequency Vibrational Spectroscopy. *Journal of the American Chemical Society* **130**, 7686-7694, doi:10.1021/ja8011116 (2008).

4 Cyran, J. D. *et al.* Molecular hydrophobicity at a macroscopically hydrophilic surface. *Proceedings of the National Academy of Sciences* **116**, 1520, doi:10.1073/pnas.1819000116 (2019).

5 Isaienko, O. & Borguet, E. Hydrophobicity of Hydroxylated Amorphous Fused Silica Surfaces. *Langmuir* **29**, 7885-7895 (2013).

6 Dalstein, L., Potapova, E. & Tyrode, E. The elusive silica/water interface: isolated silanols under water as revealed by vibrational sum frequency spectroscopy. *Physical Chemistry Chemical Physics* **19**, 10343-10349, doi:10.1039/C7CP01507K (2017).

7 Schneider, C. A., Rasband, W. S. & Eliceiri, K. W. NIH Image to ImageJ: 25 years of image analysis. *Nature methods* **9**, 671-675 (2012).

8 Stalder, A. F. *et al.* Low-bond axisymmetric drop shape analysis for surface tension and contact angle measurements of sessile drops. *Colloids and Surfaces A: Physicochemical and Engineering Aspects* **364**, 72-81, doi:https://doi.org/10.1016/j.colsurfa.2010.04.040 (2010).

9 Ho, T. A., Papavassiliou, D. V., Lee, L. L. & Striolo, A. Liquid water can slip on a hydrophilic surface. *Proceedings of the National Academy of Sciences* **108**, 16170, doi:10.1073/pnas.1105189108 (2011).

10 Kerisit, S. N. & De Yoreo, J. J. Effect of Hydrophilicity and Interfacial Water Structure on Particle Attachment. *The Journal of Physical Chemistry C* **124**, 5480-5488, doi:10.1021/acs.jpcc.9b12053 (2020).

11 Megias-Alguacil, D., Tervoort, E., Cattin, C. & Gauckler, L. J. Contact angle and adsorption behavior of carboxylic acids on α-Al2O3 surfaces. *Journal of Colloid and Interface Science* **353**, 512-518, doi:https://doi.org/10.1016/j.jcis.2010.09.087 (2011).